

# Study of differentially expressed genes related to plant height and yield in two alfalfa cultivars based on RNA-seq

Jiangjiao Qi<sup>1</sup>, Xue Yu<sup>1</sup>, Xuzhe Wang<sup>1</sup>, Fanfan Zhang<sup>1</sup>, Chunhui Ma<sup>Corresp. 1</sup>

<sup>1</sup> College of Animal Science & Technology, Shihezi University, Shihezi, Xinjiang, China

Corresponding Author: Chunhui Ma  
Email address: chunhuima@126.com

**Background.** Alfalfa (*Medicago sativa* L.) is a kind of forage with high relative feeding value in farming and livestock breeding, and is of great significance to the development of animal husbandry. The growth of the aboveground part of alfalfa is an important factor that limits crop yield. Clarifying the molecular mechanisms that maintain vigorous growth in alfalfa may contribute to the development of molecular breeding for this crop.

**Methods.** Here, we evaluated the growth phenotypes of five cultivars of alfalfa (WL 712, WL 525HQ, Victoria, Knight 2 and Aohan). Then RNA-seq was performed on the stems of WL 712, chosen as a fast growing cultivar, and Aohan, chosen as a slow growing cultivar. GO enrichment analysis was conducted on all differentially expressed genes (DEGs).

**Result.** Among the differentially expressed genes that were up-regulated in the fast-growing cultivar, GO analysis revealed enrichment in the following seven categories: formation of water-conducting tissue in vascular plants, biosynthesis and degradation of lignin, formation of the primary or secondary cell wall, cell enlargement and plant growth, cell division and shoot initiation, stem growth and induced germination, and cell elongation. KEGG analysis showed that differentially expressed genes were annotated as being involved in plant hormone signal transduction, photosynthesis, and phenylpropanoid biosynthesis. KEGG analysis also showed that up-regulated in the fast-growing cultivar were members of the *WRKY* family of transcription factors related to plant growth and development, members of the *NAC* and *MYB* gene families related to the synthesis of cellulose and hemicellulose, and the development of secondary cell wall fibres, and finally. *MYB* family members that are involved in plant growth regulation. Our research results not only enrich the transcriptome database of alfalfa, but also provide valuable information for explaining the molecular mechanism of fast-growth, and can provide reference for the production of alfalfa.

1 **Study of differentially expressed genes related to plant height and yield in two alfalfa**  
2 **cultivars based on RNA-seq**

3  
4 Jiangjiao Qi, Yuxue, Xuzhe Wang, Fanfan Zhang and Chunhui Ma

5 College of Animal Science & Technology, Shihezi University, Shihezi, 832003, Xinjiang, China

6 Corresponding Author:

7 Chunhui Ma

8 Shihezi University, Shihezi, 832003, Xinjiang, China

9 E-mails: chunhuima@126.com

10 **Abstract**

11 **Background.** Alfalfa (*Medicago sativa* L.) is a kind of forage with high relative feeding  
12 value in farming and livestock breeding, and is of great significance to the development of  
13 animal husbandry. The growth of the aboveground part of alfalfa is an important factor that  
14 limits crop yield. Clarifying the molecular mechanisms that maintain vigorous growth in alfalfa  
15 may contribute to the development of molecular breeding for this crop.

16 **Methods.** Here, we evaluated the growth phenotypes of five cultivars of alfalfa (WL 712,  
17 WL 525HQ, Victoria, Knight 2 and Aohan). Then RNA-seq was performed on the stems of WL  
18 712, chosen as a fast growing cultivar, and Aohan, chosen as a slow growing cultivar. GO  
19 enrichment analysis was conducted on all differentially expressed genes (DEGs).

20 **Result.** Among the differentially expressed genes that were up-regulated in the fast-  
21 growing cultivar, GO analysis revealed enrichment in the following seven categories: formation  
22 of water-conducting tissue in vascular plants, biosynthesis and degradation of lignin, formation  
23 of the primary or secondary cell wall, cell enlargement and plant growth, cell division and shoot  
24 initiation, stem growth and induced germination, and cell elongation. KEGG analysis showed  
25 that differentially expressed genes were annotated as being involved in plant hormone signal  
26 transduction, photosynthesis, and phenylpropanoid biosynthesis. KEGG analysis also showed  
27 that up-regulated in the fast-growing cultivar were members of the *WRKY* family of  
28 transcription factors related to plant growth and development, members of the *NAC* and *MYB*  
29 gene families related to the synthesis of cellulose and hemicellulose, and the development of  
30 secondary cell wall fibres, and finally, *MYB* family members that are involved in plant growth  
31 regulation. Our research results not only enrich the transcriptome database of alfalfa, but also  
32 provide valuable information for explaining the molecular mechanism of fast-growth, and can  
33 provide reference for the production of alfalfa.

34  
35 **Key words:** *Medicago sativa*, RNA – seq, DEGs, Stem elongation, Vigorous-growing, Slow-  
36 growing

## 42 Introduction

43 The stem is an important vegetative organ between the root and leaf of a plant and  
44 transports nutrients and water (Ernest et al., 2020). The stems of alfalfa also play a role in  
45 photosynthesis, nutrient storage, and regeneration (Pablo & Miguel, 2018). In the process of  
46 stem growth and development, stem tips grow continuously, whereas branches, leaves, and  
47 lateral branches are produced successively, which together constitute a huge branch system (Yu  
48 et al., 2015; Jaykumar & Mahendra, 2016). The degree of stem development is closely related  
49 to the life cycle of plants (Sophia et al., 2021), especially the aboveground biomass of the plant  
50 (Kleyer et al., 2019). Alfalfa, with stems and branches as the main components of biomass yield,  
51 is a typical representative crop.

52 Alfalfa is a feed crop with a high economic value (Kumar et al., 2018). In addition to its  
53 stress resistance properties, it has been the focus of research because of its perennial nature and  
54 high nutritional value (Wang et al., 2017; Diatta, Doohong & Jagadish, 2021). The stems and  
55 leaves of alfalfa have a high nutrient content and are the main parts areas of animal forage (Sulc  
56 et al., 2021). Owing to the cross-pollination of alfalfa, most cultivars have a complex genetic  
57 background. Restricted by its genetic characteristics, growth performance and nutritional  
58 quality are uneven (Bambang et al., 2021). Alfalfa stalks are composed of nodes and internodes,  
59 which affect plant height and yield. The height and stem diameter of alfalfa are important  
60 factors that restrict its biomass (Monirifar, 2011). Therefore, increasing the number of alfalfa  
61 vegetative branches, vegetative growth time, and delaying the flowering time of plants are  
62 crucial for improving the nutritional quality and yield of forage grass (Aung et al., 2015).

63 Previous studies have reported significant differences in alfalfa plant height and biomass  
64 yield among cultivars (Ziliotto et al., 2010). The series of WL alfalfa cultivars had the best  
65 growth performance when compared among cultivars (Tetteh & Bonsu, 1997). Plant spacing  
66 and light significantly effect alfalfa forage yield and weed inhibition (Celebi et al., 2010).  
67 Compound fertilizers can increase the nutrient content of soil and improve the yield of alfalfa  
68 (Iryna, Rudra & Doohong, 2021; Na et al., 2021). Additionally, the growth and development  
69 periods of alfalfa are equally important for its yield (Martin et al., 2010). During the growth of  
70 alfalfa, the budding stage ~~that~~ has excellent nutritional quality and biomass yield ~~has~~ always  
71 been a period of concern for breeders (Fan et al., 2018). Currently, research on the growth  
72 performance of alfalfa mainly focuses on the physiological level. Few reports have revealed the  
73 molecular mechanism of alfalfa stem elongation and diameter enlargement.

74 Owing to the lack of a complete reference genome sequence, previous studies on the stress-  
75 response genes of alfalfa have used nonparametric transcriptome analysis (Yuan et al., 2020;  
76 Wang et al., 2021; Gao et al., 2016; Arshad, Gruber & Hannoufa et al., 2018). Reference-free  
77 transcriptome refers to the sequencing of eukaryotic transcriptomes in the absence of a  
78 reference genome. After obtaining the original data for eukaryotic nonparametric transcriptome  
79 sequencing, the quality control splicing is first performed to generate unigenes, which are then  
80 used as the reference sequence for subsequent analysis. However, with the availability of whole-  
81 genome sequencing and annotation of alfalfa (Zhongmu 1), studying the alfalfa genome has  
82 become easier (Zhang et al., 2021).

83 Transcriptome sequencing is the study of all mRNAs present in a given sample, which is  
84 the basis for the study of gene function and is important for understanding the development of

85 organisms. With the advantages of high-throughput, high accuracy, and high sensitivity, RNA-  
86 seq can be used to study changes in the expression level of transcripts to understand or reveal  
87 the intrinsic relationship between gene expression and biological phenotypes. At present, RNA-  
88 seq technology has become a common method to study the growth and development of many  
89 plants (Chen et al., 2020; Kim et al., 2021; Zheng et al., 2021). Next-generation high-throughput  
90 sequencing technology can be used to comprehensively obtain the transcript information of  
91 alfalfa and screen out ~~the significantly different~~ genes related to stem elongation and diameter  
92 enlargement.

93 The growth rate of alfalfa is an important factor ~~of alfalfa~~ that affects plant height and  
94 yield (Yan et al., 2021). Exploring the molecular mechanisms in alfalfa that regulate growth  
95 rate may be helpful to improve yield. Here, identified differentially expressed genes (DEGs) in  
96 the stem of alfalfa "WL 712" (USA, Fall Dormancy = 10.2) and "Aohan" (China, Fall  
97 Dormancy = 2.0) using RNA-seq, further identified ~~the~~ key genes influencing vigorous-  
98 growing alfalfa by bioinformatics analysis and predicted their functions. These results may be  
99 helpful in clarifying the molecular mechanism that regulate growth rate in alfalfa, establishing  
100 a regulatory network of the growth and development of dominant cultivars, and laying a  
101 theoretical foundation for molecular breeding and the introduction of productive cultivars.

102

## 103 **Materials & Methods**

### 104 **Characterisation of phenotypic traits**

105 Five cultivars of alfalfa, *Medicago sativa* L. (WL 712, Victoria, WL 525HQ, Knight 2, and  
106 Aohan) were planted at the experimental station of Shihezi University, Xinjiang, China (N44 °  
107 20 ', E88 ° 30', altitude 420 m) (**Table S1a**). Its characteristic is temperate continental arid  
108 climate, with an average annual temperature of 8.1°C. Before planting, we adopted the "S"  
109 shaped sampling method, and nine soil samples were obtained. The nutrient status of the soil  
110 (20 cm) was as follows: available nitrogen 92.6 mg/kg, organic matter 12.4 g/kg, available  
111 potassium 168.5 mg/kg, available phosphorus 33.2 mg/kg, and pH 7.26 (**Table S1b**).

112 In June 2019 and 2020, alfalfa was planted in a 40 m<sup>2</sup> plot using a completely randomised  
113 design. To ensure consistency among the cultivars, thirty-six stems were collected from ~~the~~  
114 well-growing single plant of each cultivar. Single-row planting method was used with sampling  
115 plant spacing of 40 cm and row spacing of 60 cm, with three biological replicates per cultivar.  
116 At the budding stage, agronomic traits of five randomly selected plants were determined from  
117 each of the three biological replicates. The absolute distance from the root to the top of the main  
118 stem was measured as plant height by using a ruler. The number of branches and nodes was  
119 counted. The stem diameter and internode length were measured by using calipers. The leaf  
120 area was measured by using a leaf area meter. Five plants in each row were randomly selected  
121 and weighed, and the average value was calculated as the total fresh weight per plant. By  
122 comparing and analyzing the growth indexes of different varieties, it was finally determined  
123 that WL 712 represented a vigorous and fast-growing variety and Aohan represented a short  
124 and slow-growing variety (**Fig. 1**).

### 125 **Cultivation of experimental materials and sample collection**

126 Stems of WL 712 and Aohan were collected and cut into 8 cm pieces, leaving an axillary  
127 bud. The stems were cultivated on cutting beds in the greenhouse (light/dark: 16 h / 8 h, Temp:  
128 25 °C / 20 °C, humidity 70%) of the Beiyuan campus of Shihezi University for 20 days, and

129 surviving plants were transplanted into plastic pots (diameter 32 cm, height 35 cm). Nutrient  
130 soil: vermiculite = 1: 1 (cultivation and management methods were consistent). More than 30  
131 individual plants of both WL 712 and Aohan survived in the greenhouse. Five plants each of  
132 WL 712 and Aohan alfalfa were randomly selected and the plant height, internode length, stem  
133 diameter, leaf area and yield were determined.

134 At the budding stage (about 42 days after transplanting), the plant height of WL 712 and  
135 Aohan reached 50.2 cm and 28.7 cm (**Table 1**), respectively. We collected the main stem and  
136 removed its top and base. The middle part of the main stem (~~cut into~~ approximately 1.5 cm) of  
137 each cultivar was collected, quickly frozen in liquid nitrogen. Three biological replicates were  
138 used for per cultivar. WJ1, WJ2 and WJ3 represent samples from the WL 712 cultivar. AJ1,  
139 AJ2 and AJ3 represent samples from the Aohan cultivar. Finally, six samples were used for  
140 RNA-seq.

#### 141 **Library construction and RNA-seq**

142 Total RNA was isolated from stems using the RNeasy Plant Mini Kit (Qiagen, Germany).  
143 A total of 3 µg RNA per sample was used to build the library. Sequencing libraries were  
144 generated using a NEBNext Ultra RNA Library Prep Kit (NEB, USA). Messenger RNA was  
145 purified from each sample using magnetic beads and fragmented with divalent cations at  
146 elevated temperature. First-strand cDNA was obtained using segmented mRNA as template and  
147 random oligonucleotide as primer. Then, the second strand of cDNA was obtained in a DNA  
148 polymerase I system. The double-stranded cDNA was purified using AMPure XP Beads  
149 (Beckman Coulter, Beverly, USA). The double-stranded cDNA was ligated to the sequencing  
150 adaptor after terminal repair and A tail, and 250-300 bp cDNA was obtained using AMPure XP  
151 beads. Finally, the PCR system was amplified, and the PCR products were purified again using  
152 AMPure XP beads to obtain the libraries.

153 Library quality was examined using the Agilent Bioanalyzer 2100 system. The effective  
154 concentration of the library ( $\geq 2$  nM) was quantified using qRT-PCR. After passing the  
155 inspection, the libraries were pooled and sequenced on the Illumina HiSeq X-10 (California,  
156 USA) platform by Beijing Novo Biotech Company, Ltd. Finally, each sample contained an  
157 average of 6.63 G of valid data, and  $4.42 \times 10^7$  clean reads.

#### 158 **Quality control**

159 To ensure the accuracy of data analysis, we filtered the original data and examined the  
160 sequencing error rate. Using in-house Perl scripts to process the raw reads of fastq  
161 format. Removing reads containing adapters, ploy-N sequences, and low-quality from the raw  
162 data to obtain clean reads. The Q20, Q30, and GC contents of the clean data were calculated. All  
163 subsequent analyses depend on clean data, high quality.

#### 164 **RNA-seq data analysis**

165 The analysis and calculation of all transcriptome data referred to previous research report  
166 (Trapnell et al., 2012). In brief, the index of the reference genome was constructed using  
167 HISAT2 v2.2.1. The paired-end clean reads were obtained using HISAT2 v2.2.1  
168 (<https://cloud.biohpc.swmed.edu/index.php/s/fE9QCsX3NH4QwBi/download>) aligned to the  
169 reference genome Zhongmu No. 1  
170 ([https://figshare.com/articles/dataset/genome\\_fasta\\_sequence\\_and\\_annotation\\_files/12327602](https://figshare.com/articles/dataset/genome_fasta_sequence_and_annotation_files/12327602)) to  
171 obtain mapped reads (Mortazavi, Williams & McCue, 2008). We also analysed the proportion  
172 of mapped reads in the exons, introns, and intergenic regions of the genome.

173 The clean reads aligned to Zhongmu No. 1 were quantified using FeatureCounts v1.5.0-  
174 p3. Gene expression was tested by FPKM (fragments per kilobase of transcript per million  
175 fragments mapped), and differences between WL 712 and Aohan FPKM values were compared  
176 using FeatureCounts v1.5.0-p3.

177 Differential expression analysis of the two comparison combinations was performed using  
178 the DESeq2 R package (1.16.1)  
179 (<https://www.bioconductor.org/packages/release/bioc/html/DESeq2.html>). DESeq2 determines the  
180 differential expression in digital gene expression data using a model based on a negative  
181 binomial distribution. The corrected P-values and  $|\log_2\text{foldchange}|$  are thresholds for significant  
182 differential expression. P-values were adjusted using the Benjamini & Hochberg method.

183 Gene Ontology (GO) (<http://www.geneontology.org/>) enrichment and KEGG (Kyoto  
184 Encyclopedia of Genes and Genome) (<http://www.genome.jp/kegg/>) statistical analysis of DEGs  
185 were performed using the clusterProfiler R package. A corrected P-value less than 0.05 was  
186 used as the threshold for significant enrichment of differentially expressed genes.

### 187 qRT-PCR

188 The accuracy of the RNA-seq was verified by qRT-PCR. Total RNA was isolated from  
189 stems, and cDNA was synthesised by using the PrimeScript RT reagent Kit (Takara, Tokyo,  
190 Japan). Alfalfa  $\beta$ -Actin 2 was used as the internal gene. The primers in **Table S2** were used for  
191 qRT-PCR. qRT-PCR was completed using the LightCycler 96/LightCycler480 system. The  
192 solution of the 20  $\mu$ L system contained 0.4  $\mu$ L forward primer, 0.4  $\mu$ L reverse primer, 10  $\mu$ L TB  
193 Green Fast qPCR Mix (2X) (Takara, Tokyo, Japan) and 2 ng cDNA. The PCR procedure  
194 included 45 cycles, with 3 technical repeats for each reaction. According to Kenneth report,  
195 the relative expression of each gene was calculated (Livak & Schmittgen, 2001).

### 196 Statistical Analysis

197 All statistical analysis was using SPSS software (version 17; IBM Inc, USA). The data  
198 were compared using Student's t-test, and  $P < 0.05$  was considered statistically significant. The  
199 power of our samples was calculated using RNASeqPower  
200 (<https://bioconductor.org/packages/release/bioc/html/RNASeqPower.html>), and the RNASeqpower  
201 was 94.2%.

202  
203  
204  
205  
206  
207  
208  
209  
210  
211  
212  
213  
214  
215  
216

217 **Results**218 **Phenotypic analysis of five alfalfa varieties**

219 To compare the differences in the growth patterns of the five cultivars (**Table S1a**), plant  
220 height, internode length and stem diameter of alfalfa at different growth stages were continually  
221 measured in 2019 and 2020 (**Fig. 2, Table S3**). There were no significant differences in plant  
222 height, internode length or stem diameter among cultivars at the seedling transplant stage. After  
223 the budding stage, plant height, internode length and stem diameter of different alfalfa varieties  
224 reached a plateau and remained relatively stable (**Fig. 2a-c**). In 2019 and 2020, WL 712 and  
225 Aohan represented tall and short phenotypes, respectively (**Fig. 2d**). Comparing the agronomic  
226 traits of alfalfa at the budding stage in 2019 and 2020, the plant height of WL 712 was  
227 approximately 1.78 and 1.91 times those of Aohan, respectively, and the stem diameter of WL  
228 712 was approximately 1.90 and 1.92 times those of Aohan (**Fig. 2d-e**). The internode length  
229 and number of lateral branches in WL 712 were significantly larger than those in Aohan ( $P <$   
230  $0.01$ ), whereas the number of main branches in WL 712 was significantly lower ( $P < 0.05$ ) (**Fig.**  
231 **2f, Fig. 3a-b**).

232 To identify the correlation between internode length and stem diameter and other traits,  
233 the fresh weight, leaf-stem ratio, and dry weight of the five cultivars were also determined. The  
234 results showed that the production performances of WL 712 and Aohan were significantly  
235 different ( $P < 0.05$ ) (**Fig. 3c-f**). Phenotypic correlation analysis based on 8 agronomic traits was  
236 done. We found that fresh and dry weight were positively and strongly correlated with the  
237 number of lateral branches, plant height, stem diameter, and internode length, and plant height  
238 was significantly positively correlated with internode length ( $P < 0.01$ ). In addition, the number  
239 of main branches was negatively correlated with plant height, stem diameter, and internode  
240 length ( $P < 0.01$ ) (**Table 2**).

241 From the screening of five alfalfa cultivars, WL 712 and Aohan were identified as the  
242 cultivars with the most significant difference in growth performance (**Fig. 1**). The growth trend  
243 of the two varieties in greenhouse is similar to that in field. The plant height, internode length,  
244 yield per plant, leaf area and stem diameter of WL 712 alfalfa were significantly higher than  
245 those of Aohan alfalfa (**Table 2**).

246 Based on the above results, WL 712 and Aohan were used as the vigorous-growing and  
247 slow-growing experimental cultivars, ~~while the stem base tissue with the budding stage (the~~  
248 ~~surviving plants were transplanted and planted for about 42 days) was used for RNA-seq.~~

249 **RNA-seq analysis**

250 Using RNA-seq, we obtained  $2.74 \times 10^8$  raw reads. The sequence error rate of a single  
251 base position was 0.03%, and the average GC content was 41.65%. After filtering from the raw  
252 data,  $2.65 \times 10^8$  (96.94%) clean reads (39.76 G) were obtained. The phred values were greater  
253 than 97% and 93% at  $Q_{20}$  and  $Q_{30}$ , respectively (**Table S1c**). The Pearson coefficient showed  
254 that the homology among the samples within the group was higher than 84.6% (**Fig. S1**).

255 We aligned the clean reads with the reference genome. The average proportions of exons,  
256 introns and intergenic regions in AJ samples were 72.72%, 3.61%, and 23.67%, respectively.  
257 Similarly, the WJ samples accounted for 74.14%, 2.96%, and 22.90%, respectively (**Table S4**).  
258 The reads aligned to the intron region may have been derived from the precursor mRNA. The  
259 reads aligned to the intergenic region may have been derived from ncRNAs.

260 Additionally, according to the comparison of RNA-seq data from WL 712 and Aohan, the

261 RNASeq power of our sample was 94.2%. The result may be beneficial to screen and explore  
262 the functional DEGs related to the vigorous-growing of alfalfa. These results demonstrated that  
263 the experiments were reproducible and that the data were accurate.

#### 264 **Identification and functional annotation of DEGs in WL 712 and Aohan**

265 Generally, the gene expression value of RNA-seq is evaluated as fragments per kilobase  
266 of transcript per million mapped reads (FPKM), which corrects the sequencing depth and gene  
267 length ~~successfully~~ (Fig. S2). More than 90% of the clean reads were successfully mapped to  
268 the alfalfa genome. To clarify the function of the DEGs between WL 712 and Aohan, we  
269 performed GO and KEGG enrichment analyses. In total, 954 DEGs were significantly enriched  
270 and assigned to 35 GO terms. Compared to Aohan, WL 712 upregulated 578 genes and  
271 downregulated 376 genes. Among the molecular function, “*protein heterodimerization activity*”  
272 [GO:0046982] (114 DEGs, 11.95%) was the highest proportion, followed by “*UDP-*  
273 *glycosyltransferase activity*” [GO:0008194] (99 DEGs, 1.04%) and “*translation factor activity,*  
274 *RNA binding*” [GO:0008135] (86 DEGs, 9.01%). Among the cell components, “*bounding*  
275 *membrane of organelle*” [Go:0098588] (57 DEGs, 5.97%) represented the largest cluster,  
276 followed by “*whole membrane*” [Go:0098805] (49 DEGs, 5.13%) and “*peptidase complex*”  
277 [Go:1905368] (44 DEGs, 4.61%). Among the biological processes, “*translational elongation*”  
278 [GO:0006414] (41 DEGs, 4.30%) represented the largest cluster (Table 3, Table S5, Fig. 4).

279 Based on biological system network, the function of DEG was identified using KEGG  
280 classification. A total of 1324 genes were enriched in 110 KEGG pathways (Fig. 5). “*Carbon*  
281 *metabolism*” [ath01200] (103 DEGs, 7.8%) and “*Ribosome*” [ath03010] (96 DEGs, 7.3%) were  
282 the most abundant pathways; followed by “*Biosynthesis of amino acids*” [ath01230] (81 DEGs,  
283 6.1%), “*RNA transport*” [ath03013] (54 DEGs, 4.1%), “*Plant-pathogen interaction*” [ath04626]  
284 (52 DEGs, 3.9%), “*Protein processing in endoplasmic reticulum*” [ath04141] (52 DEGs, 3.9%)  
285 and “*Plant hormone signal transduction*” [ath04075] (44 DEGs, 3.2%) (Table S6).

#### 286 **Expression and regulation of DEGs in WL 712 and Aohan**

287 KEGG analysis showed that DEGs related to stem elongation and diameter enlargement  
288 were widely involved in biological processes such as hormone signalling, photosynthesis and  
289 transcriptional regulation (Table S7).

290 Plant hormone signal transduction (Ath04075) involves many hormones that regulate the  
291 growth and development, such as auxins, cytokinins, gibberellins, brassinosteroids, jasmonic  
292 acid, and ethylene. Twelve DEGs were enriched in the auxin-mediated signalling pathway,  
293 including *auxin-responsive protein SAUR* (SAUR), *auxin-induced protein X10A* (new gene) and  
294 *auxin transporter-like protein LAX*. Among these, IAA9, IAA6, SAUR50, SAUR32 and  
295 SAUR36 were significantly upregulated. In the cytokinin-mediated signalling pathway, four  
296 DEGs were enzyme genes, such as *adenylate isopentenyltransferase 5* (IPT5), *7-*  
297 *deoxyloganetin glucosyltransferase* (UGT85A24), *cytokinin dehydrogenase 6* (CKX6), and  
298 *cytokinin hydroxylase* (CYP735A2). *DELLA protein GAI* (GAI), *f-box protein GID2* (GID2),  
299 and *transcription factor PIF4* (PIF4) were enriched in the gibberellin-mediated signalling  
300 pathway. *Serine/threonine-protein kinase BSK8* (BSK8), *serine/threonine-protein kinase BSK1*  
301 (BSK1), and *Cyclin-D3-3* (CYCD3-3) were enriched in the brassinosteroid-mediated signalling  
302 pathway. Five DEGs were enriched in the jasmonic mediated signalling pathway, including  
303 *Coronatine-insensitive protein homolog 1a* (COIIA), *Protein TIFY 6 B* (TIFY6B), *Protein TIFY*  
304 *11 B* (TIFY11B), *Protein TIFY 10 B* (TIFY10B) and *Protein TIFY 3 B* (TIFY3B). Four



305 upregulated DEGs were enriched in the ethylene-mediated signalling pathway, including  
306 *ethylene receptor (ETR1)*, *mitogen-activated protein kinase kinase 4 (MKK4)*, *mitogen-*  
307 *activated protein kinase homolog MMK1 (MMK1)*, and *protein ethylene insensitive 3 (EIN3)*.

308 Fifteen DEGs were enriched in the photosynthetic pathway (ath00195). Among them,  
309 *PPL1*, *PETC*, *PSBR*, *PSBS*, *PSAG*, *PSAO*, *PSB 27* and *PSB 28* were related to the photoreaction.  
310 *PLSN 2* was related to the activity of the chloroplast NAD(P)H dehydrogenase (NDH) complex.  
311 *ATPF 2* and *ATPC* are related to ATPase activity. Additionally, two oxygen-evolving enhancer  
312 proteins and ferredoxins have been identified. In the photosynthesis-antenna protein (ath00196)  
313 pathway, eleven DEGs were classified into *chlorophyll a-b binding proteins* and *chlorophyll*  
314 *a/b binding proteins*, which were expressed in chloroplasts. In the MAPK signalling (ath04016)  
315 pathway, twenty-two DEGs were mainly involved in biotic stress (pathogen infection), abiotic  
316 stress (cold/salt/drought/osmotic stress), and hormone synthesis during root growth and  
317 wounding responses.

318 Furthermore, the TCA cycle (ath00020), carbon fixation in photosynthetic organisms  
319 (ath00710), glycolysis/gluconeogenesis (ath00010), ribosome (ath03010), amino sugar and  
320 nucleotide sugar metabolism (ath00520), pyruvate metabolism (ath00620), and  
321 phenylpropanoid biosynthesis (ath00940) appeared closely related to alfalfa growth (**Table S7**).  
322 In the TCA cycle pathway, 12 DEGs are annotated as playing a role in catalysis of the pyruvate  
323 dehydrogenase complex. In addition, *ATP-citrate synthase alpha chain protein 1 (ACLA1)* and  
324 *2 malate dehydrogenases (MDH)* were identified. *Pyrophosphate--fructose 6-phosphate 1-*  
325 *phosphotransferase subunit beta (PFK)* and *glycolaldehyde-3-phosphate dehydrogenase*  
326 *(GAPC1)*, both members of the glycolysis/gluconeogenesis pathway were highly expressed.  
327 Seven *glyceraldehyde-3-phosphate dehydrogenase (GAPDH)* genes were enriched in the  
328 “carbon fixation in the photosynthetic organism” pathway and were highly expressed.  
329 Ribosomal proteins predominated in the ribosomal pathway and included proteins that are parts  
330 of the 30S subunit (*RPS1*, *RPS13*, *RPSQ*, *RPS16*), 40S subunit (*RP24a*, *RP30a*, *RP15d*, *RP10a*,  
331 *RP20a*), 50S subunit (*RPL28*, *RPMJ*, *RPL31*, *RPLX*) and 60S subunit (*RPP3a*, *RPL21e*,  
332 *RPL37a*, *RPL37B*). *Dihydrolipoyllysine-residue acetyltransferase component 2 of the pyruvate*  
333 *dehydrogenase complex* (putative ortholog of *At3g13930*) and *malate dehydrogenase (mMDH)*  
334 were highly expressed among the pyruvate metabolic pathway genes. *Beta-glucosidase 44*  
335 (*BGLU44*), *beta-amylase 1 (BAM1)*, *acid beta-fructofuranosidase (VCINV)*, and *probable*  
336 *fructokinase-4 (At3g59480)* were highly expressed among genes in the starch and sucrose  
337 metabolism pathways. The genes the phenylpropanoid biosynthesis pathway with high  
338 expression were *Probable cinnamyl alcohol dehydrogenase (CAD2)*, *beta-glucosidase 46*  
339 (*BGLU46*), *trans-cinnamate 4-monooxygenase (CYP73A3)*, and *3 peroxidases (PER)*.

#### 340 **DEGs enriched in a variety of biological processes**

341 All DEGs were analysed using GO and KEGG analyses. We found ~~that~~ seven groups of  
342 DEGs plausibly related to stem elongation and diameter expansion, including formation of  
343 water-conducting tissue in vascular plants, cell division and shoot initiation, biosynthesis and  
344 degradation of lignin, cell enlargement and plant growth, formation of the primary or secondary  
345 cell wall, cell elongation, and stem growth and induced germination (**Table S8**). Fourteen DEGs  
346 were enriched in lignin biosynthesis and degradation. Peroxidases play an important role in this  
347 process. Additionally, *peroxidase 47 (PER47)* is a novel gene (**Fig. 6a**). Eleven DEGs were  
348 enriched in the formation of the primary or secondary cell wall class. *Cellulose synthase A*

349 *catalytic subunit (CESA)* is up-regulated in WL 712 (**Fig. 6b**). Eighteen DEGs were enriched  
350 in the cell enlargement and plant growth category. AUXs, such as *auxin-responsive protein*  
351 (*IAA9*), *auxin-induced protein (IAA6)* and *auxin transporter-like protein (LAX5)*, were  
352 particularly abundant. Additionally, *auxin-induced protein X10A* is a novel gene (**Fig. 6c**). Five  
353 DEGs were enriched in the cell division and shoot initiation category. Enzyme genes such as *7-*  
354 *deoxyloganetin glucosyltransferase (UGT85A24)*, *cytokinin hydroxylase (CYP735A2)* and  
355 *cytokinin dehydrogenase 6 (CKX6)* were particularly abundant (**Fig. 7a**). Two DEGs were  
356 enriched in the stem growth and induced germination category. Interestingly, one them, *DELLA*  
357 *protein (GAI)*, is argued to negatively regulate the gibberellin signalling pathway, whereas the  
358 other, *F-Box protein (GID2)*, is supposed to regulate that pathway positively (**Fig. 7b**).  
359 *Serine/threonine-protein kinase (BSK 1)* and *BSK8* are thought to be related to cell elongation  
360 (**Fig. 7c**). *Eukaryotic translation initiation factor 5A-1 (EIF5A)*, *mitogen-activated protein*  
361 *kinase kinase kinase 3 (ANP3)*, and *alpha, alpha-trehalose-phosphate synthase (TPS6)* are  
362 apparently involved in the formation of water-conducting tissues (**Fig. 7d**). Additionally, we  
363 identified genes that are thought to regulate senescence, including *protein ethylene insensitive*  
364 *3 (EIN3)* (**Fig. 6d**). Importantly, compared with Aohan, *cellulose synthase A catalytic subunit*  
365 *8 (CESA8)*, *beta-1,4-xylosyltransferase (IRX 9)*, *probable beta-1,4-xylosyltransferase (IRX*  
366 *14H)*, *auxin-responsive protein (SAUR36)*, *peroxidase 16 (PER16)*, and *peroxidase 51 (PER51)*  
367 were upregulated more than 8-fold in WL 712, whereas *mitogen-activated protein kinase 3*  
368 (*MPK3*), *pathogenesis-related protein (At2g14610)*, *peroxidase 55 (POD55)*, *beta-glucosidase*  
369 *46 (BGLU46)*, and *peroxidase 15 (POD15)* were downregulated more than 15-fold in WL  
370 712 (**Table S9**). All the genes that might be related to stem growth and development were  
371 clustered together, as shown in **Fig. 6** and **Fig. 7**.

### 372 **Transcription factors potentially involved in alfalfa growth and development**

373 Transcription factors are essential in plant growth and development as protein molecules  
374 that regulate gene expression. In this study, 20 transcription factors were implicated in the  
375 difference between fast and slow growing alfalfa cultivars (**Fig. 8a, Table S10**). Seven DEGs  
376 were upregulated, including *NAC domain-containing protein 73 (NAC073)*, *NAC domain-*  
377 *containing protein 10 (NAC010)*, *transcription factor MYB 46 (MYB46)*, and *NAP-related*  
378 *protein 2 (NRP2)*. Additionally, *WRKY transcription factor 22 (WRKY22)*, *transcription factor*  
379 *TGA 1 (TGA1)* and *transcription factor MYB86* were novel genes. GO annotations state that  
380 *NAC073* and *NAC010* are involved in the synthesis of cellulose and hemicellulose and the  
381 development of secondary cell wall fibres. Thirteen DEGs were downregulated, and the *WRKY*  
382 and *MYB* family members were conspicuous among them. GO classification state that *WRKY51*  
383 is involved in the positive regulation of salicylic acid-mediated signal transduction and negative  
384 regulation of jasmonic acid-mediated signal transduction in the defense response. *WRKY54* is  
385 apparently a negative regulator of plant growth and development. *MYB46* is apparently involved  
386 in secondary wall cellulose synthesis as a transcriptional activator. Finally, *MYB86* is apparently  
387 involved in lignin synthesis and accumulation. Additionally, *MYB2* is known to inhibit the  
388 expression of light-harvesting genes. All identified transcription factors were validated using  
389 qRT-PCR (**Fig. 8b**). The relative expression of *NAC081* was significantly upregulated in WL  
390 712 plant ( $P < 0.001$ ). The relative expression levels of most transcription factors were similar  
391 to the FPKM trend.

### 392 **The reliability of RNA-seq was verified using qRT-PCR**

393 To determine the accuracy and rationality of the data, we arbitrarily selected 11 DEGs for  
394 qRT-PCR validation. The chosen DEGs were mainly related to the formation of the primary or  
395 secondary cell wall, cell enlargement and plant growth, and synthesis and degradation of lignin.  
396 The changes in transcript abundance are shown in **Fig. 9a**. qRT-PCR revealed that *IRX9*, *CESA8*,  
397 *CESA7*, *MKK4*, *PER16*, and *PER51* were significantly upregulated in WL 712 plant ( $P < 0.05$ ).  
398 *MPK3*, *At2g14610*, *BGLU46*, and *POD15* were significantly downregulated in WL 712 ( $P <$   
399  $0.05$ ) (**Fig. 9b**). However, the relative expression of *CAD2* between the two varieties was not  
400 significantly different ( $P > 0.05$ ) and was inconsistent with the RNA-seq transcript abundance.  
401 This may have been caused by RNA-seq errors in the acceptable range. Overall, the relative  
402 expression trend of the DEGs was similar to the RNA-seq.

403

## 404 Discussion

405 Alfalfa is an important component of feed, and the growth performance of its aboveground  
406 part affects the biomass yield. The *FmS6K* gene plays an important role in regulating the  
407 development of plant stems (Sun et al., 2018). The yield of elephant grass has a strong positive  
408 correlation with internode length (Yan et al., 2021). However, the molecular regulatory  
409 mechanisms underlying the growth rate of stems and branches in alfalfa remain unclear. In this  
410 study, the growth difference between the tall and fast-growing variety WL 712 and the short  
411 and slow-growing variety Aohan was studied. The transcriptome of those two varieties was  
412 analyzed by RNA-seq, with RNA obtained from the ~~stem base~~. The difference between qRT-  
413 PCR and RNA-seq of individual DEGs may be caused by the error of RNA-seq within the  
414 acceptable range. Overall, the RNA-seq data could be used for subsequent analysis. All DEGs  
415 were associated with at least one GO term; 954 significant DEGs were obtained, and seven  
416 DEG clusters were speculated to be involved in promoting fast growth (**Fig. 6**, **Fig.7**).  
417 Additionally, KEGG revealed that hormone signal transduction, photosynthesis and  
418 phenylpropanoid biosynthesis genes are up-regulated in the faster growing cultivar. RNA-seq  
419 also identified several novel DEGs associated with the fast growing cultivar, including *PER47*  
420 and *TIFY10A*.

421 Plant organ growth is influenced by both developmental processes and environmental  
422 factors (Sun et al., 2018). In many cases, these changes are due to hormone-mediated action  
423 (Verma, Ravindran & Kumar, 2016). ~~In this study~~, auxin, cytokinin, gibberellin, ethylene,  
424 brassinosteroid, and jasmonic acid were all implicated because their downstream targets were  
425 found among DEGs, such as *SAUR50*, *CKX6*, *GID 2*, and *GAI*. These DEGs might play a role  
426 in promoting fast growth in alfalfa. Previous studies have identified *SAURs* as a class of  
427 hormones that regulate plant growth and development and promote cell enlargement (Ren &  
428 Gray, 2015). Cytokinin synthesis is required to activate shoot division in apple trees with the  
429 top removed (Tan et al., 2018). Relevant studies have shown that gibberellin regulates plant  
430 organ elongation and development (Nagel, 2020). *GAI* is an inhibitor of highly conserved  
431 gibberellin signalling in plants. The *SCF (GID2)* complex mediates degradation of DELLA  
432 proteins (*RLG2*, *RGA*, and *GAI*), and activates and positively regulates the gibberellin signalling  
433 pathway (Dill et al., 2004). In addition, in the plant hormone signal transduction pathway, the  
434 production of hormones that play a mediating role depends on the metabolism of amino acids  
435 or fatty acids. Tryptophan in plants is not only involved in the synthesis of proteins but also the  
436 precursor of many metabolites (such as auxin) (Manol & Nemoto, 2012). Jasmonic acid induces

437 plants to prioritise defense over growth by interfering with the gibberellin signalling cascade,  
438 which is usually accompanied by significant growth inhibition (Yang et al., 2012). *TIFY*, which  
439 encodes jasmonic acid repressor, was significantly upregulated in Aohan (**Table S7**). This may  
440 explain why the Aohan alfalfa is a dwarf plant.

441 Photosynthesis is an essential metabolic process. Twenty-nine DEGs were related to  
442 photosynthesis. For example, *PIF 1* and *PIF 3* were significantly downregulated in WL 712  
443 (**Table S7**). These genes may play a regulatory role in the process of plant height and internode  
444 elongation. Plant height and leaf area of transgenic soybean are decreased by overexpressing  
445 *PIF4* (Arya, Singh & Bhalla, 2021). The deletion of *PIF1* and *PIF3* results in an increase in  
446 plant height, longer internodes, and late flowering (Hoang et al., 2021). The light-harvesting  
447 complex II (LHC II) functions as a light receptor and is related to the absorption of light (Gu et  
448 al., 2017; Sen et al., 2021). The up-regulation of LHC II DEGs may enhance the photosynthesis  
449 of WL 712 and promote the growth of plants. Additionally, circadian rhythm is also involved  
450 in the regulation of plant growth and development (Venkat & Muneer, 2022). Our research  
451 found that DEGs enriched in circadian rhythm pathway were mainly related to photoperiod  
452 flowering response. (**Table S7**).

453 RNA-seq analysis found 1531 DEGs related to rape stem growth (Yuan et al., 2019).  
454 Combined analysis of proteome and RNA-seq found that DEGs and DEPs of *Mikania*  
455 *micrantha* stems were significantly enriched in photosynthesis, carbon sequestration and plant  
456 hormone signal transduction pathways (Can et al., 2021). We identified seven DEG clusters  
457 that were plausibly involved in stem elongation and enlargement. Fourteen DEGs were  
458 annotated as being involved in lignin synthesis and degradation and peroxidases (**Fig. 6a**).  
459 These genes may regulate lignin synthesis and degradation in stems. The oxidation activity of  
460 peroxidases is important for lignification (Hoffmann et al., 2020). Eleven DEGs were  
461 apparently involved the formation of the primary or secondary cell wall (**Fig. 6b**), with good  
462 representation from cellulose synthase. Previous studies reported that *CESA 4* and *CESA8* are  
463 specifically enriched and expressed in the stem tissue during the fiber development stage (Guo  
464 et al., 2021). Eighteen DEGs were enriched in the category of cell enlargement and plant growth  
465 (**Fig. 6c**) frequently involving auxin. Five DEGs were apparently involved in cell division and  
466 shoot initiation (**Fig. 7a**). Two DEGs were enriched in the categories of stem growth and  
467 induced germination (**Fig. 7b**), mainly components of the gibberellin signalling pathway. Two  
468 DEGs were potentially involved in cell elongation (**Fig. 7c**). These DEGs might play a role in  
469 stem internode elongation, diameter enlargement and lateral branch formation. Previous studies  
470 reported that *AtTPS6* completely compensates for the defects in reduced trichome and stem  
471 branching due to *csp-1* deficiency in *Arabidopsis thaliana* (Chary et al., 2008). Deletion of  
472 *IAA17* in tomatoes showed that the increase in fruit size is related to the higher ploidy level of  
473 peel cells (Su et al., 2015). Finally, the *TIFY* homologs possibly involved in senescence were  
474 also identified here (**Fig. 6d**). In addition, we identified several members of *SPL* family, such  
475 as *SPL1*, *SPL6* and *SPL7*, which may be involved in the lateral branch development of alfalfa.  
476 Previous studies reported that *SPL13* regulates shoot branching in alfalfa (Gao et al., 2018).  
477 Overall, these DEGs may be involved in alfalfa growth and development.

478 Transcription factors are essential in the regulation of development, morphogenesis and  
479 responses to environmental stress. Previous research found that most members of *NAC*, *WRKY*  
480 and *MYB* families are involved in the synthesis of lignin, cellulose, and hemicellulose (Wang

et al., 2016). The *NAC*-mediated transcription network synergistically regulates synthesis of the plant secondary wall (Ryan, Zhong & Ye, 2011). *WRKY6* and *WRKY33* positively regulated abscisic acid signal transduction during early development of *A. thaliana* (Huang et al., 2016). *WRKY54* is a negative regulator of salicylic acid synthesis (Li, Zhong & Palva, 2017) and can significantly increase stem diameter, leaf area, and total dry weight of plants (Amin et al., 2013). Overexpression of *AtMYB44* in tomatoes results in slow growth (Shim et al., 2012). *MYB3R1* is a transcriptional repressor that regulates organ growth, and restricts plant growth and development by binding to target genes and promoters of specific genes (Wang et al., 2018). Under reduced light intensity, *MYB2* and *MYR1* act as inhibitors of flowering and organ elongation, respectively (Zhao et al., 2011). Here, excluding *WRKY22*, all *WRKY* members were significantly upregulated in dwarf alfalfa. Therefore, *WRKY22* may positively regulate the growth and development of WL 712. *NACs* are involved in the development of plant secondary cell walls. Among these, *NAC081* functions as a positive regulator. *MYB46* and *MYB86* might positively regulate the synthesis of cellulose and lignin, and *MYB44*, *MYB3R1* and *MYB2* might act as transcriptional repressors (**Table S10**).

### Conclusion

Plant height is an important factor in determining forage biomass. The molecular characteristics of the DEGs between fast and slow growing alfalfa cultivars were identified using RNA-seq. The trend of our qRT-PCR was largely consistent with those of RNA-seq, which indicated that the RNA-seq data could be used for subsequent analysis. All DEGs were analysed using GO terms, and 954 significant DEGs were identified. KEGG analysis indicated that hormone signal transduction, phenylpropanoid biosynthesis, and photosynthesis are well represented in the fast growing cultivar. GO analysis highlighted the following seven clusters of DEGs: formation of water-conducting tissue, cell division and shoot initiation, synthesis and degradation of lignin, stem growth, formation of the primary or secondary cell wall, cell enlargement and plant growth, and induced germination and cell elongation. Additionally, the transcription factors implicated in stem elongation and diameter expansion are mainly *WRKY*, *NAC*, and *MYB* family members. In summary, our research results not only enrich the transcriptome database of alfalfa, but also provide valuable information for explaining the molecular mechanism of fast growth, and can provide reference for the production of alfalfa around the world.

### Competing Interests

The authors declare there are no competing interests.

### Author Contributions

Qi Jiangjiao conceived and designed the experiments, performed the experiments, analyzed the data, prepared figures or tables, and authored or reviewed drafts of the paper.

Yuxue, Wang Xuzhe and Zhang Fanfan performed the experiments.

Ma Chunhui conceived and designed the experiments, performed the experiments, analyzed the data, authored or reviewed drafts of the paper, and approved the final draft.

### Availability of data and materials

The data is available at the Sequence Read Archive (SRA) of NCBI: <https://www.ncbi.nlm.nih.gov/sra/?term=PRJNA807394>.

### Funding

This work was supported by China Agriculture Research System of MOF and MARA.

525 **Reference**

- 526 Aung B, Gruber M, Amyot L, Omari K, Bertrand A, Hannoufa A. 2015. Ectopic expression of  
527 LjmiR156 delays flowering, enhances shoot branching, and improves forage quality in  
528 alfalfa. *Plant Biotechnology Reports* 9(6):379-393
- 529 Arshad M, Gruber MY, Hannoufa A. 2018. Transcriptome analysis of microRNA156  
530 overexpression alfalfa roots under drought stress. *Scientific Reports* 8:9363
- 531 Arya H, Singh MB, Bhalla PL. 2021. Overexpression of PIF4 affects plant morphology and  
532 accelerates reproductive phase transitions in soybean. *Food and Energy Security* 10(3):1
- 533 Amin AA, El-Kader AA Abd, Shalaby MAF, Gharib FAE, Rashad ESM, Teixeira da SJA. 2013.  
534 Physiological effects of salicylic acid and thiourea on growth and productivity of maize  
535 plant in sandy soil. *Communications in Soil Science & Plant Analysis* 44(7):1141-1155
- 536 Bambang S, Lukmana A, Nafiatul U, Bambang S. 2021. The performance and genetic variation  
537 of first and second generation tropical alfalfa (*Medicago sativa*). *Biodiversitas* 22(6):3265-  
538 3270
- 539 Celebi SZ, Kaya L, Sahar AK, Yergin R. 2010. Effects of the weed density on grass yeild of  
540 alfalfa in different row spacing applications. *African Journal of Biotechnology* 9(41):6867-  
541 6872
- 542 Chen L, Yang Y, K Mishina, Cui C, Zhao Z, Duan S, Chai Y, Su R, Chen F, Hu Y.G. 2020.  
543 RNA-seq analysis of the peduncle development of Rht12 dwarf plants and primary mapping  
544 of Rht12 in common wheat. *Cereal Research Communications* 48(2):139-14
- 545 Cui C, Wang Z, Su YJ, Wang T. 2021. New insight into the rapid growth of the *Mikania*  
546 *micrantha* stem based on DIA proteomic and RNA-seq analysis. *Journal of Proteomics* 236:  
547 104126
- 548 Chary SN, Hicks GR, Choi YG, Carter D, Raikhel NV. 2008. Trehalose-6-phosphate  
549 synthase/phosphatase regulates cell shape and plant architecture in Arabidopsis. *Plant*  
550 *Physiology* 146(1):97-107
- 551 Diatta AA, Doohong M, Jagadish SVK. 2021. Drought stress responses in non-transgenic and  
552 transgenic alfalfa--current status and future research directions. *Advances in Agronomy*  
553 170:35-100
- 554 Dill A, Thomas SG, Hu JH, Steber CM, Sun TP. 2004. The Arabidopsis F-box protein  
555 SLEEPY1 targets gibberellin signaling repressors for gibberellin-induced degradation.  
556 *Plant Cell* 16(6):1392-1405
- 557 Ernest BA, Alena PB, Mariam RS, Marian O, Edo G, Henk VA, Richard GFV, C Gerard VDL.  
558 2020. Morphological and physiological responses of the potato stem transport tissues to  
559 dehydration stress. *Planta* 251(2):45
- 560 Etzold S, Sterck F, Bose AK, Braun S, Buchmann N, Eugster W, Gessler A, Kahmen A, Peters  
561 RL, Vitasse Y, Walthert L, Ziemińska Kasia, Zweifel R, Penuelas J. 2021. Number of  
562 growth days and not length of the growth period determines radial stem growth of temperate  
563 trees. *Ecology Letters* 25:427– 43
- 564 Fan WQ, Ge GT, Liu YH, Wang W, Liu LY, Jia YS. 2018. Proteomics integrated with  
565 metabolomics: analysis of the internal causes of nutrient changes in alfalfa at different  
566 growth stages. *BMC Plant Biology* 18 (1):78
- 567 Gao RM, Austin RS, Amyot L, Hannoufa A. 2016. Comparative transcriptome investigation of  
568 global gene expression changes caused by miR156 overexpression in *Medicago sativa*.

- 569 *BMC Genomics* 17(1):658
- 570 Guo JD, Huang Z, Sun JL, Cui XM, Liu Y. 2021. Research progress and future development  
571 trends in medicinal plant transcriptomics. *Frontiers in Plant Science* 12:691838
- 572 Gu JF, Zhou ZX, Li ZK, Chen Y, Wang ZQ, Zhang H, Yang JC. 2017. Photosynthetic properties  
573 and potentials for improvement of photosynthesis in pale green leaf rice under high light  
574 conditions. *Frontiers in Plant Science* 8:1082
- 575 Hoang QTN, Tripathi S, Cho JY, Choi DM, Shin AY, Kwon SY, Han YJ, Kim JI. 2021.  
576 Suppression of phytochrome interacting factors enhance photoresponses of seedlings and  
577 delays flowering with increased plant height in brachypodium distachyon. *Frontiers in*  
578 *Plant Science* 12:756795
- 579 Hoffmann N, Benske A, Betz H, Schuetz M, Samuels AL. 2020. Laccases and peroxidases co-  
580 localize in lignified secondary cell walls throughout stem development. *Plant Physiology*  
581 184(2):806-822
- 582 Huang Y, Feng CZ, Ye Q, Wu WH, Chen YF. 2016. Arabidopsis WRKY6 transcription factor  
583 acts as a positive regulator of abscisic acid signaling during seed germination and early  
584 seedling development. *PLoS Genetics* 12(2):e1005833
- 585 Jaykumar JC, Mahendra LA. 2016. In vitro callus induction and plant regeneration from stem  
586 explants of ceropia noorjahaniae, a critically endangered medicinal herb. *Methods in*  
587 *Molecular Biology* 1391:347-355
- 588 Kleyer M, Trinogga J, Cebrin-Piqueras MA, Trenkamp A, Fljgaard C, Ejrnas R, Bouma TJ,  
589 Minden V, Maier M, Mantilla CJ, Albach DC, Blasius B, Barua D. 2019. Trait correlation  
590 network analysis identifies biomass allocation traits and stem specific length as hub traits  
591 in herbaceous perennial plants. *Journal of Ecology* 107(2):829-842
- 592 Kumar T, Bao AK, Bao Z, Wang F, Gao L, Wang SM. 2018. The progress of genetic  
593 improvement in alfalfa (*Medicago sativa* L). *Czech Journal of Genetics and Plant Breeding*  
594 54(2):41-51
- 595 Kim S, Cho K, Lim SH, Goo TW, Lee JY. 2021. Transcriptome profiling of transgenic rice  
596 seeds lacking seed storage proteins (globulin, prolamin, and glutelin) by RNA-seq analysis.  
597 *Plant Biotechnology Reports* 15(1):77-93
- 598 Katyayani NU, Rinne PLH, Tarkowska D, Strnad M, Schoot C. 2020. Dual role of gibberellin  
599 in perennial shoot branching: inhibition and activation. *Frontiers in Plant Science* 11:736
- 600 Livak KJ, Schmittgen TD. 2001. Analysis of relative gene expression data using real-time  
601 quantitative PCR and the  $2^{-\Delta\Delta CT}$  method. *Methods* 25(4): 402-408
- 602 Li J, Zhong R, Palva ET. 2017. WRKY70 and its homolog WRKY54 negatively modulate the  
603 cell wall-associated defenses to necrotrophic pathogens in Arabidopsis. *PLoS One* 12(8):1-  
604 22
- 605 Martin N, Brink G, Shewmaker G, Undersander D, Walgenbach R, Hall M. 2010. Changes in  
606 alfalfa yield and nutritive value within individual harvest periods. *Agronomy Journal*  
607 102(4):1274-1282
- 608 Monirifar H. 2011. Path analysis of yield and quality traits in alfalfa. *Notulae Botanicae Horti*  
609 *Agrobotanici Cluj-Napoca* 39(2):190-195
- 610 Mortazavi A, Williams BA, McCue K. 2008. Mapping and quantifying mammalian  
611 transcriptomes by RNA-seq. *Nature Methods* 5(7):621-628
- 612 Manol Y, Nemoto K. 2012. The pathway of auxin biosynthesis in plant. *Journal of*

- 613 *Experimental Botany* 63:2853-2872
- 614 Nagel R. 2020. Gibberellin signaling in plants: entry of a new microRNA player. *Plant*  
615 *Physiology* 183(1):5-6
- 616 Pablo PG, Miguel AMR. 2018. Stem cells and plant regeneration. *Developmental Biology*  
617 442(1):3-12
- 618 Ren H, Gray WM. 2015. SAUR proteins as effectors of hormonal and  
619 environmental signals in plant growth. *Molecular Plant* 8(8):1153-1164
- 620 Ryan LM, Zhong RQ, Ye ZH. 2011. Secondary wall NAC binding element (SNBE), a key cis-  
621 acting element required for target gene activation by secondary wall NAC master switches.  
622 *Plant Signaling & Behavior* 6(9):1282-1285
- 623 Sulc RM, Arnold AM, Cassida KA, Albrecht KA, Hall MH, Min D, Xu X, Undersander DJ,  
624 Santen E. 2021. Changes in forage nutritive value of reduced-lignin alfalfa during regrowth.  
625 *Crop Science* 61(2):1478-1487
- 626 Sun H, Zhao XT, Liu Z, Yang K, Wang Y, Zhan YG. 2018. Bioinformatics of S6K genes in  
627 *Fraxinus mandshurica* and their expression analysis under stress and hormone. *Plant*  
628 *Research* 38(5):714-724
- 629 Sen S, Mascoli V, Liguori N, Croce R, Visscher L. 2021. Understanding the relation between  
630 structural and spectral properties of light harvesting complex II. *The Journal of Physical*  
631 *Chemistry. A* 125(0): 4313-4322
- 632 Su LY, Audran C, Bouzayen M, Roustan JP, Chervin C. 2015. The Aux/IAA, SI-IAA17  
633 regulates quality parameters over tomato fruit development. *Plant Signaling & Behavior*  
634 10(11):e1071001
- 635 Shim JS, Jung C, Lee S, Min K, Lee YW, Choi Y, Lee JS, Song JT, Kim JK, Choi YD. 2012.  
636 AtMYB44 regulates WRKY70 expression and modulates antagonistic interaction between  
637 salicylic acid and jasmonic acid signaling. *The Plant Journal* 73 (3):483-495
- 638 Trapnell C, Roberts A, Goff L, Pertea G, Kim D, Kelley DR, Pimentel H, Salzberg SL, Rinn  
639 JL, Pachter L. 2012. Differential gene and transcript expression analysis of RNA-seq  
640 experiments with TopHat and Cufflinks. *Nature Protocols* 7:562-578
- 641 Tetteh JP, Bonsu KO. 1997. Agronomic performance of seven cultivars of alfalfa (*Medicago*  
642 *sativa* L.) in the coastal savanna zone of Ghana. *Ghana Journal of Agricultural Science*  
643 30(1):39-44
- 644 Tan M, Li GF, Qi SY, Liu XJ, Chen XL, Ma JJ, Zhang D, Han MY. 2018. Identification and  
645 expression analysis of the IPT and CKX gene families during axillary bud outgrowth in  
646 apple (*Malus domestica* Borkh). *Gene* 651:106-117
- 647 Verma V, Ravindran P, Kumar PP. 2016. Plant hormone-mediated regulation of stress  
648 responses. *BMC Plant Biology* 16(1):1-10
- 649 Venkat Ajila, Muneer Sowbiya. 2022. Role of circadian rhythms in major plant metabolic and  
650 signaling pathways. *Frontiers in Plant Science* 13: 836244
- 651 Wang J, Tang F, Gao CP, Gao X, Xu B, Shi FL. 2021. Comparative transcriptome between male  
652 fertile and male sterile alfalfa (*Medicago varia*). *Physiology and Molecular Biology of*  
653 *Plants* 27(7):1487-1498
- 654 Wang YJ, Li MC, Wu Wang, Wu HY, Xu YN. 2013. Cloning and characterization of an  
655 AP2/EREBP gene TemAP2-1 from *Tetraena mongolica*. *Bulletin of Botany* 48(1):23-33
- 656 Wang HZ, Yang JH, Chen F, Torres-Jerez I, Tang YH, Wang MY, Du Q, Cheng XF, Wen JQ,  
657 Dixon R. 2016. Transcriptome analysis of secondary cell wall development in *Medicago*



- 657 *truncatula*. *BMC Genomics* 17:23
- 658 Wang WP, Sijacic P, Xu PB, Lian HL, Liu ZC. 2018. Arabidopsis TSO1 and MYB3R1 form a  
659 regulatory module to coordinate cell proliferation with differentiation in shoot and root.  
660 *Proceedings of the National Academy of Sciences of the United States of America*  
661 115(13):e3045-e3054
- 662 Yu L, Chen HW, Hong PP, Wang HL, Liu KF. 2015. Adventitious bud induction and plant  
663 regeneration from stem nodes of *Salvia splendens* 'Cailinghong'. *Hortscience* 50:869-872
- 664 Yuan JB, Sun XB, Guo T, Chao YH, Han LB. 2020. Global transcriptome analysis of alfalfa  
665 reveals six key biological processes of senescent leaves. *Peer Journal* 8(1):e8426
- 666 Yu KMJ, McKinley B, Rooney WL, Mullet JE. 2021. High planting density induces the  
667 expression of GA3-oxidase in leaves and GA mediated stem elongation in bioenergy  
668 sorghum. *Scientific Reports* 11(1):46
- 669 Yan Q, Li J, Lu LY, Gao LJ, Lai DW, Yao N, Yi XF, Wu ZY, Lai ZQ, Zhang JY. 2021. Integrated  
670 analyses of phenotype, phytohormone, and transcriptome to elucidate the mechanism  
671 governing internode elongation in two contrasting elephant grass (*Cenchrus purpureus*)  
672 cultivars. *Industrial Crops & Products* 170:113693
- 673 Yuan R, Zeng XH, Zhao SB, Wu G, Yan XH. 2019. Identification of candidate genes related to  
674 stem development in *Brassica napus* using RNA-seq. *Plant Molecular Biology Reporter*  
675 37(4):347-364
- 676 Ziliotto U, Leinauer B, Lauriault LM, Rimi F, Macolino S. 2010. Alfalfa yield and morphology  
677 of three fall dormancy categories harvested at two phenological stages in a subtropical  
678 climate. *Agronomy Journal* 102(6):1578-1585
- 679 Zhang H, Liu XQ, Wang XM, Sun M, Song R, Mao PS, Jia SG. 2021. Genome-wide  
680 identification of GRAS genes family and their responses to abiotic stress in *Medicago sativa*.  
681 *International Journal of Molecular Sciences* 22(14):7729
- 682 Zheng XM, Chen YJ, Zhou YF, Shi KK, Hu X, Li DY, Ye HZ, Zhou Y, Wang K. 2021. Full-  
683 length annotation with multistrategy RNA-seq uncovers transcriptional regulation of  
684 lncRNAs in cotton. *Plant Physiology* 185(1):179-195
- 685 Zhao CS, Atsushi H, Shinjiro Y, Kamiya Yuji, Beers EP. 2011. The Arabidopsis MYB genes  
686 MYR1 and MYR2 are redundant negative regulators of flowering time under decreased  
687 light intensity. *Plant Journal* 66(3):502-515

# Figure 1

Slow-growing Aohan and vigorous-growing WL 712 plants at bud stage.

Soil grown plants, approximately 60 days after planting.



## Figure 2

Phenotypic evaluation of five alfalfa cultivars.

The dynamics of plant height (a), stem diameter (b) and internode length (c) of five alfalfa cultivars during the indicated stages of development. Here, we recorded the transplanting stage as 0 day, branching stage (18 d), budding stage (42 d), early flower stage (45 d) and full flower stage (50 d). Average plant height (d), stem diameter (e), internode length (f) of five alfalfa cultivars. The values are the average of fifteen biological replicates and error bars represent the standard deviation. Different letters indicate significant difference at  $P < 0.05$  among the five cultivars as determined by Student's t test.

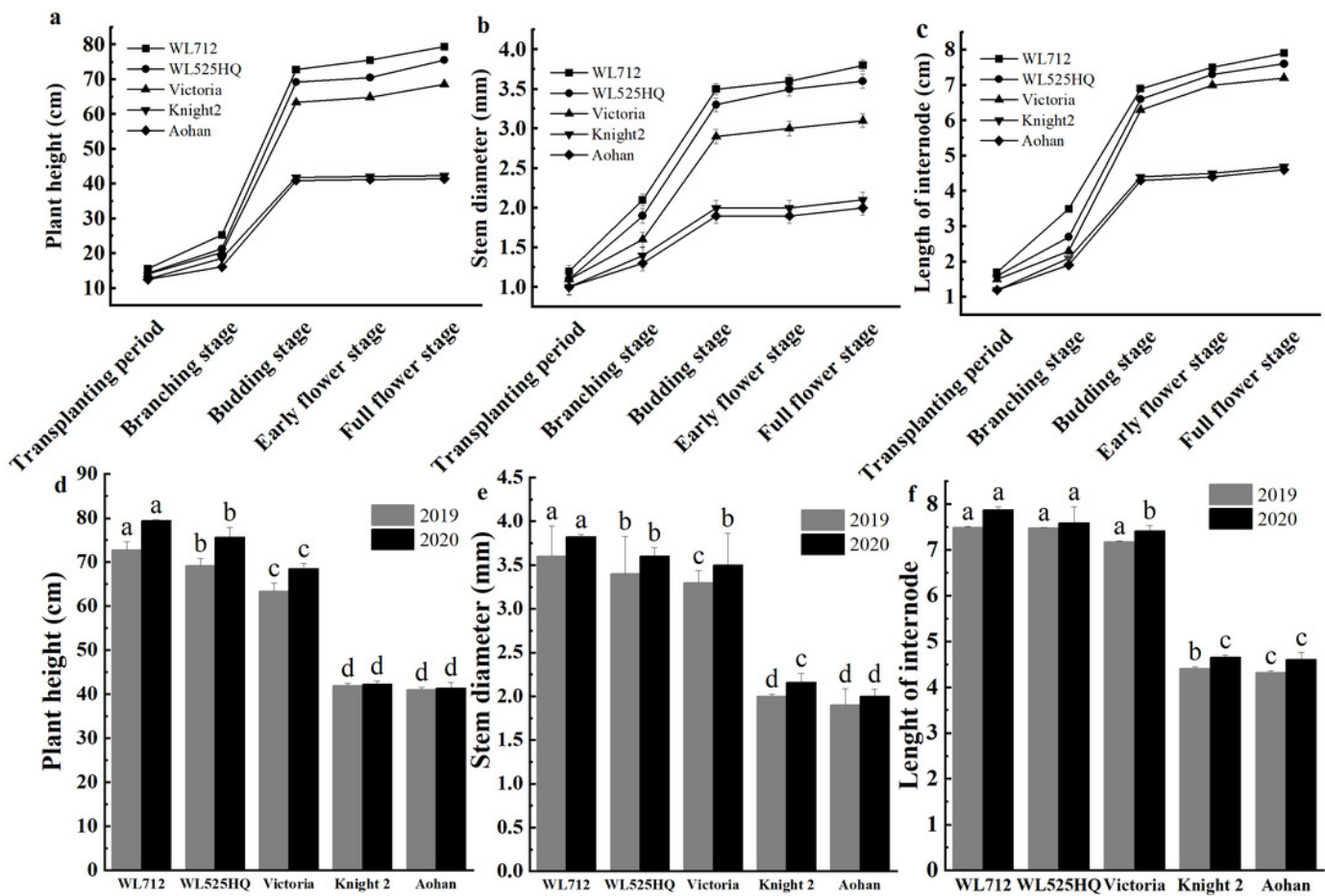


## Figure 3

Phenotypic evaluation and index determination of five alfalfa cultivars at budding stage (42 d).

Lateral branch number (a), total branch number (b), leaf area (c), fresh weight (d), leaf to stem ratio (e) and dry weight (f) of five alfalfa cultivars. The values are the average of fifteen biological replicates and error bars represent the standard deviation. Different letters indicate significant difference at  $P < 0.05$  among the five cultivars as determined by Student's t test.

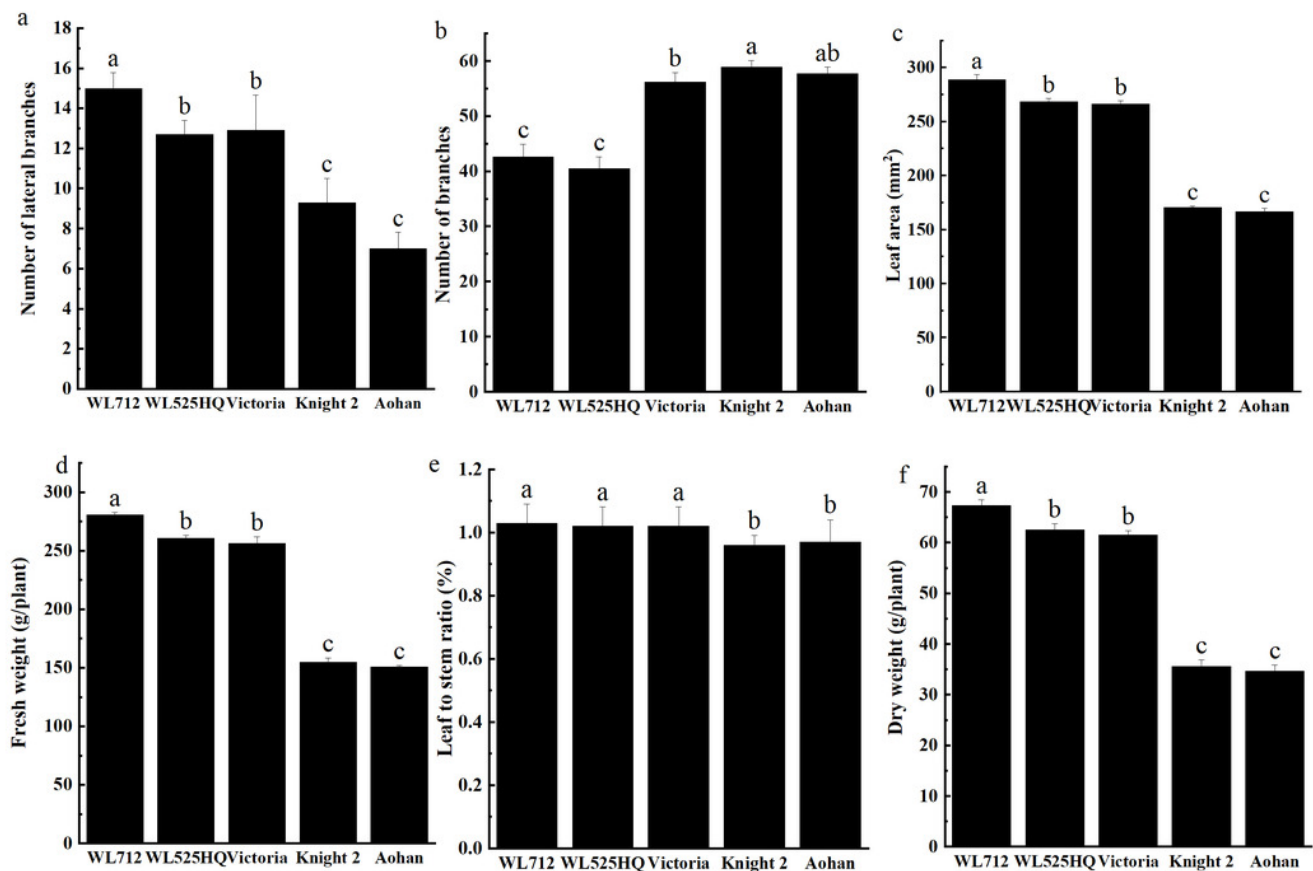


## Figure 4

Scatter diagram of enriched GO functional categories.

The “GeneRatio” shows the ratio of the number of DEGs in the given category to the total number of differentially expressed genes. The size of the spot indicates the approximate number of DEGs in the category, all the spots indicate the significance level,  $P < 0.05$ .

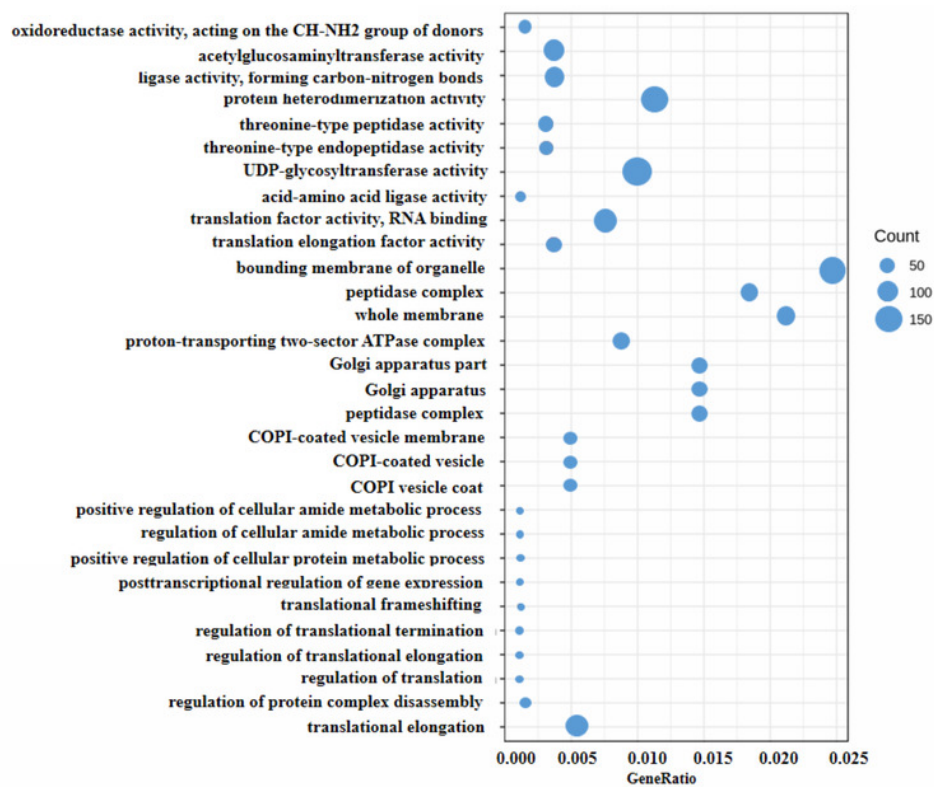


## Figure 5

KEGG classification of differentially expressed genes (DEGs).

X-axis is the number of gene annotations; Y-axis is the type of KEGG pathway.

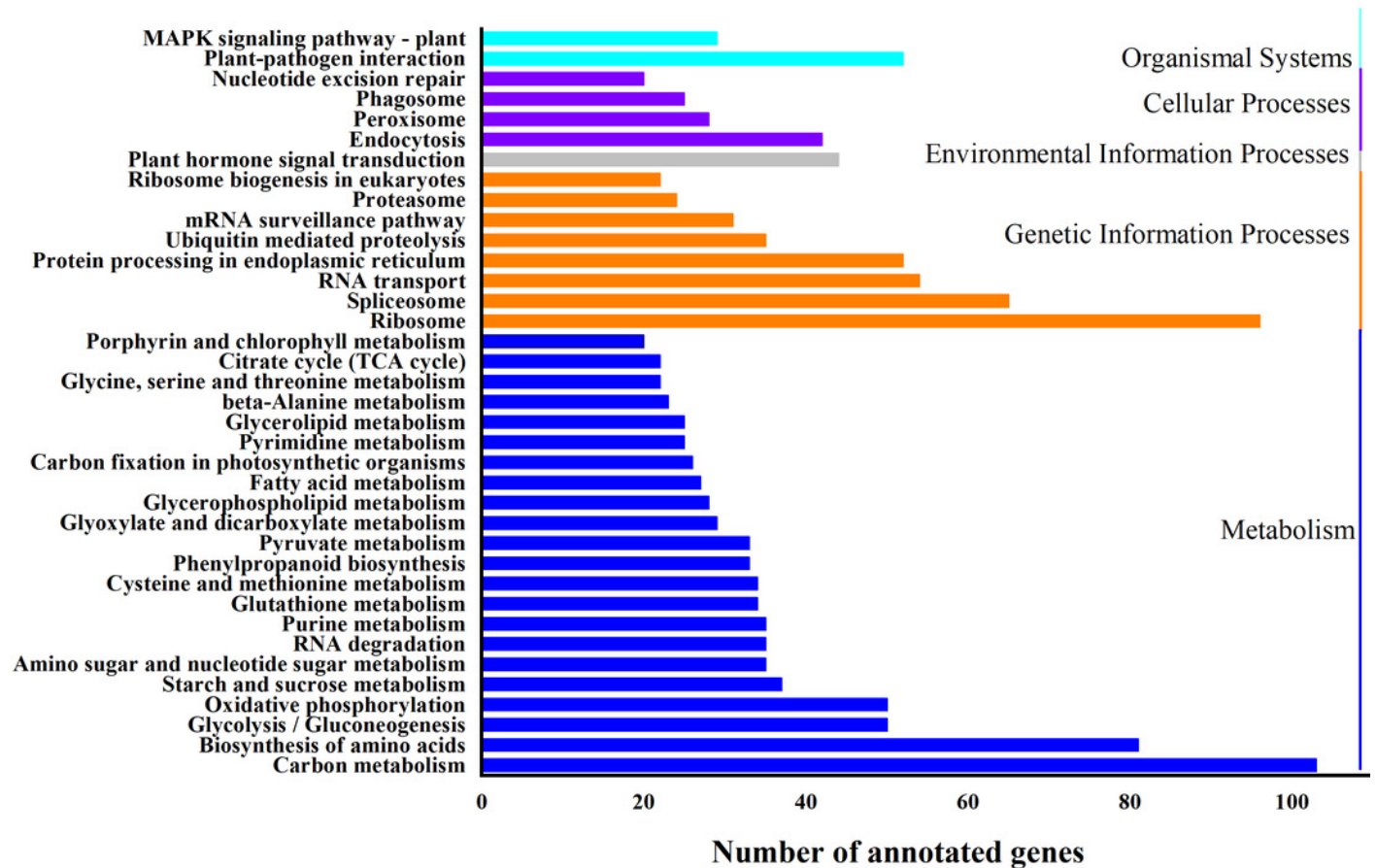


## Figure 6

Bar graphs showing the FPKM (fragments per kilobase of transcript per million mapped reads) of DEGs involved in various biological processes distinguished by GO enrichment analysis.

(a) Synthesis and degradation of lignin; (b) Formation of the primary cell wall or secondary cell wall; (c) Cell enlargement and plant growth; (d) Senescence.

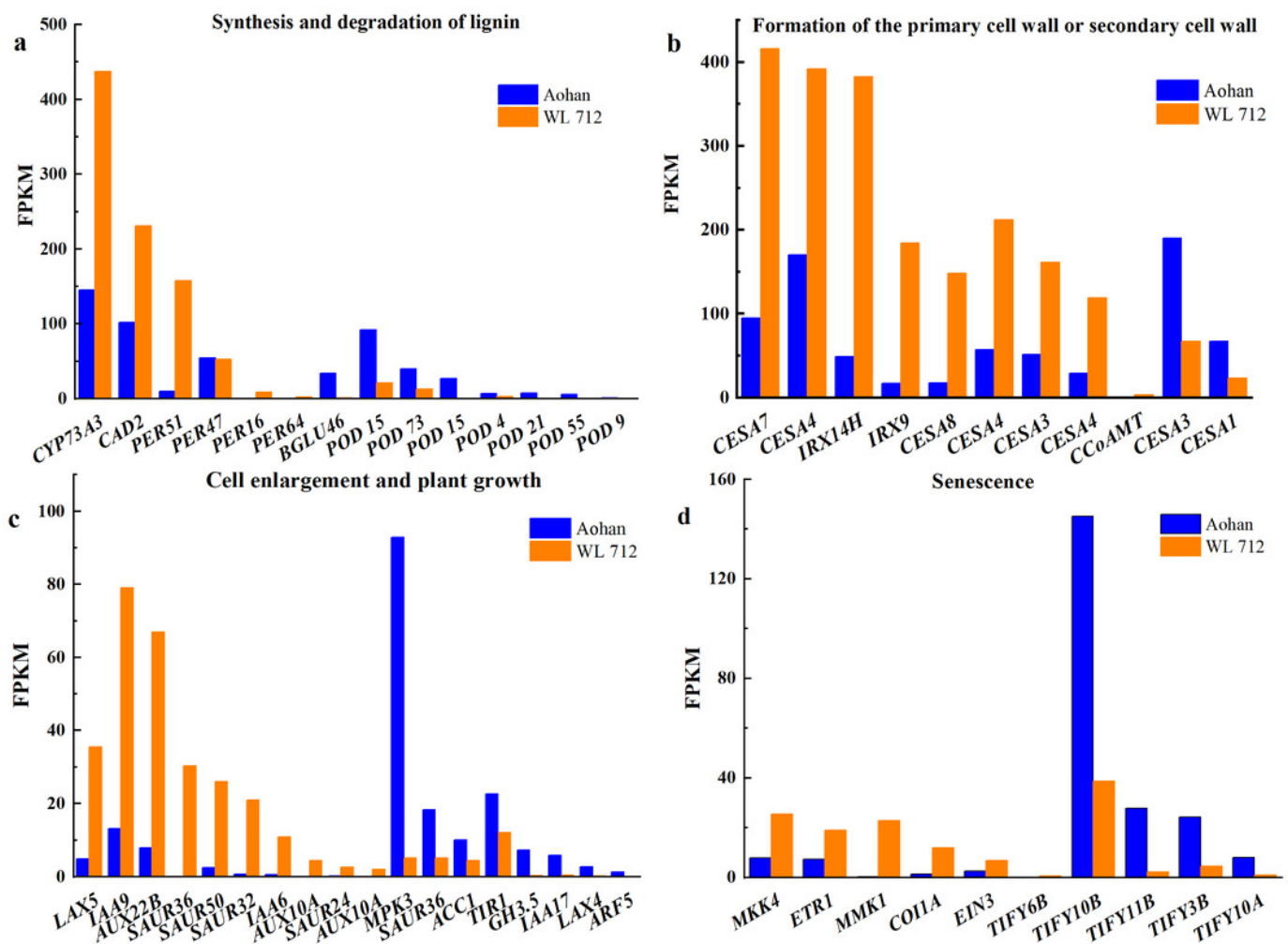




## Figure 7

Bar graphs showing the FPKM of DEGs involved in additional biological processes distinguished by GO enrichment analysis.

(a) Cell division and shoot initiation; (b) Stem growth and induced germination; (c) Cell elongation; (d) Formation of water-conducting tissues.

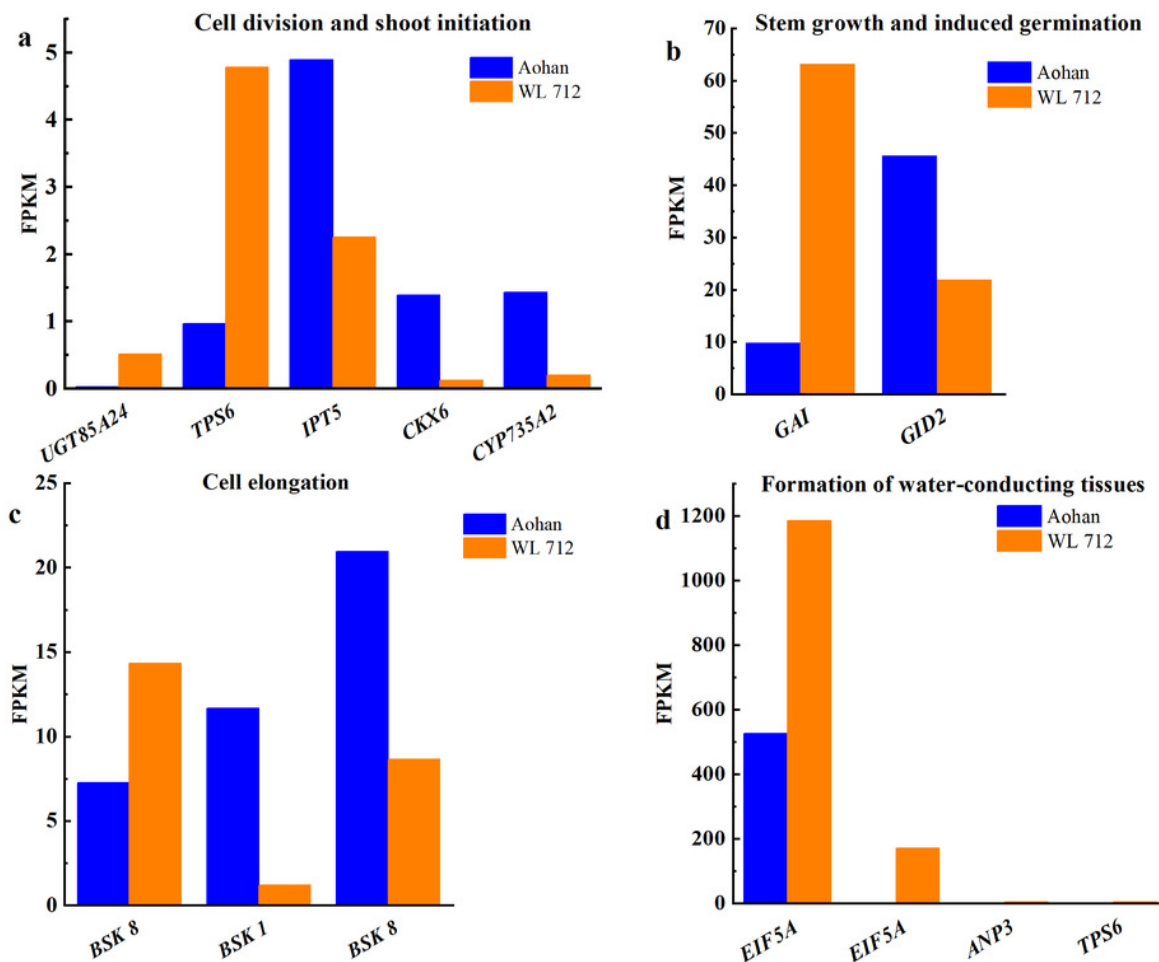


## Figure 8

Transcription factors putatively involved in stem elongation and diameter enlargement in alfalfa as distinguished by GO analysis.

(a) Bar graphs showing the transcript abundance based on FPKM. (b) Bars plot the relative expression levels based on qPCR. \*, \*\*, \*\*\* Expression level of the cultivars is significantly different at the 0.05, 0.01, and 0.001 probability levels, respectively. The expression levels of all genes were homogenized with the standard of internal reference ( $\beta$ -Actin).

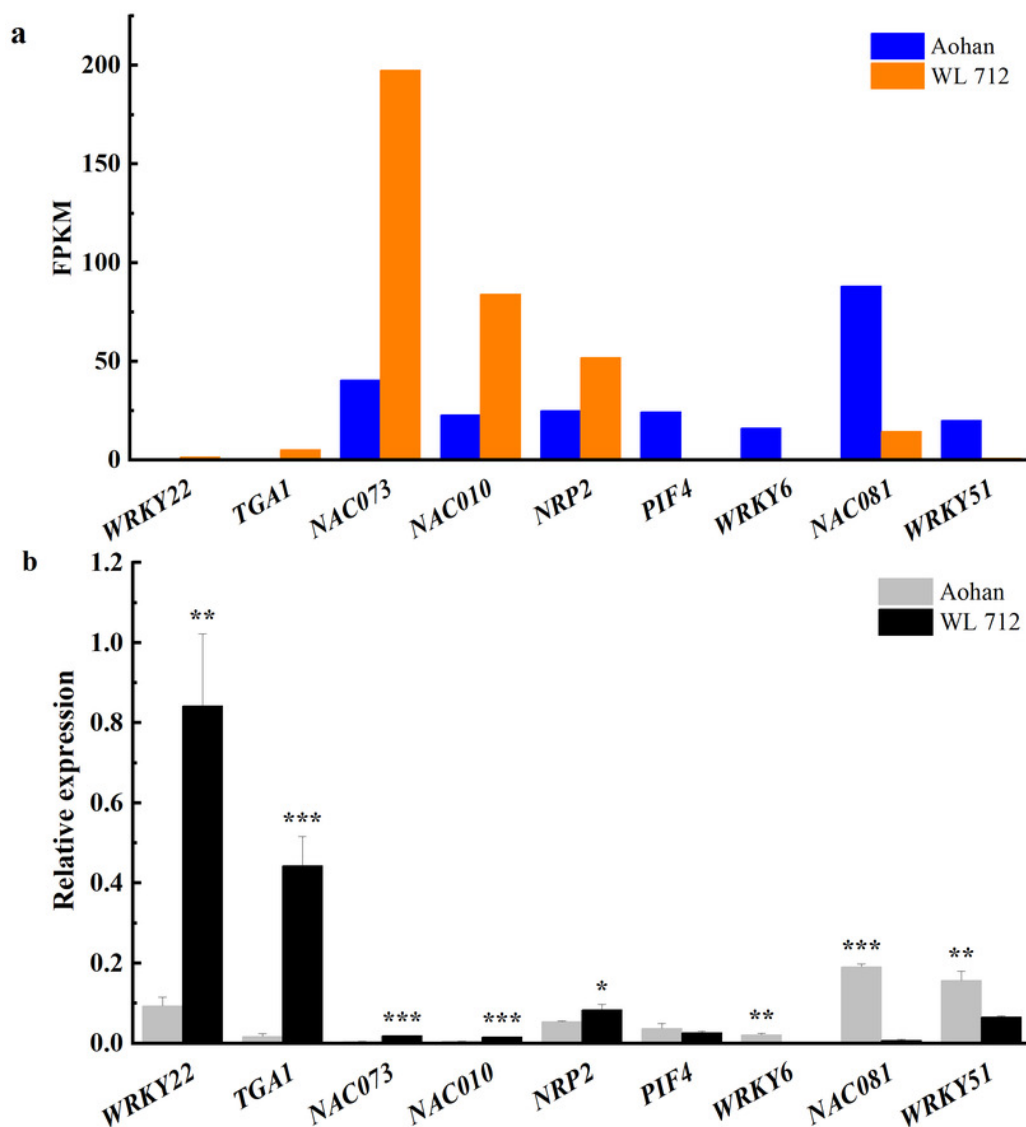


## Figure 9

Comparison of RNA-seq and qRT-PCR for 11 genes.

(a) RNAseq bars show transcript abundance based on FPKM. (b) qRT-PCR bars show the transcript abundance based on qRT-PCR. \*, \*\*\* Expression level of the cultivars is significantly different at the 0.05, and 0.001 probability levels, respectively. The expression levels of all genes were homogenized with the standard of internal reference ( $\beta$ -Actin).

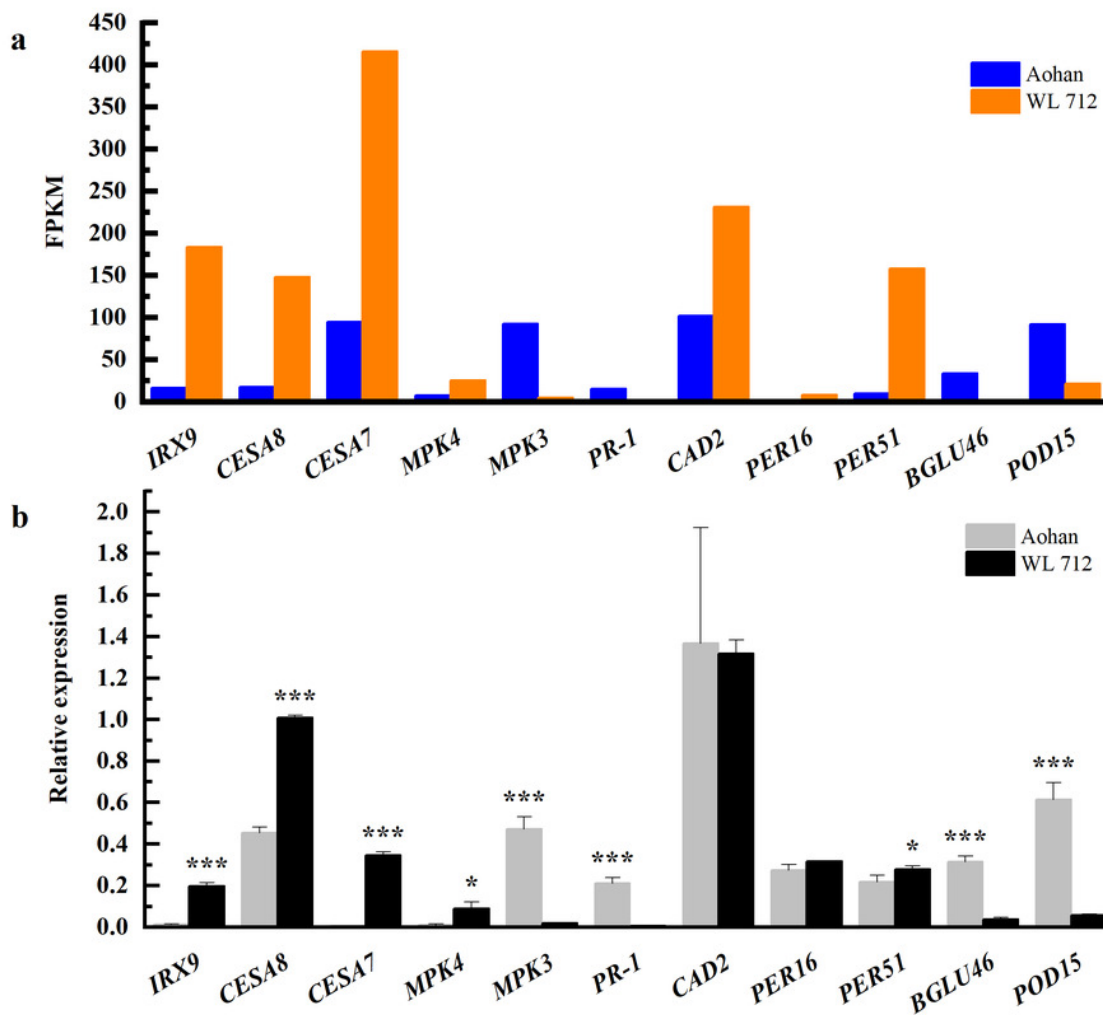


**Table 1** (on next page)

The growth index of the two varieties in greenhouse-grown plants

Different letters indicate significant difference at  $P < 0.05$  among the two varieties as determined by Student's t test.

1 Table 1 The growth index of the two varieties in greenhouse-grown plants

2

	<b>Plant Height (cm)</b>	<b>Length of Internodde (cm)</b>	<b>Stem Diameter (mm)</b>	<b>Leaf Areas (mm<sup>2</sup>)</b>	<b>Plant Weight (g/plant)</b>
<b>WL 712</b>	50.2 ± 1 <sup>a</sup>	5.14 ± 0.09 <sup>a</sup>	2.52 ± 0.022 <sup>a</sup>	159 ± 0.6 <sup>a</sup>	231 ± 2.4 <sup>a</sup>
<b>Aohan</b>	28.7 ± 1 <sup>c</sup>	2.94 ± 0.07 <sup>c</sup>	1.19 ± 0.027 <sup>c</sup>	127 ± 2.8 <sup>c</sup>	141 ± 0.4 <sup>c</sup>

3

4 Different letters indicate significant difference at  $P < 0.05$  among the two varieties as determined by Student's t test.

**Table 2** (on next page)

Correlation coefficients between traits among the five alfalfa cultivars

\*, \*\* Significant at the 0.05, and 0.01 probability levels, respectively. PH, plant height; IL, internode length; SD, stem diameter; FW, fresh weight; LSR, leaf-to-stem ratio; DW, dry weight; LBN, lateral branch number; MBN, main branch number.

1 Table 2. Correlation coefficients between traits among the five alfalfa cultivars

2

	PH	SD	IL	LBN	MBN	FW	LSR	DW
PH	1							
SD	0.98**	1						
IL	0.99**	0.98**	1					
LBN	0.89**	0.92**	0.90**	1				
MBN	-0.84**	-0.76**	-0.79**	-0.68**	1			
FW	0.98**	0.98**	0.98**	0.91**	-0.75**	1		
LSR	0.55**	0.54**	0.55**	0.51**	-0.46*	0.60**	1	
DW	0.99**	0.99**	0.99**	0.82**	-0.76**	1.00**	0.59**	1

3

4 \*, \*\* Significant at the 0.05, and 0.01 probability levels, respectively.

5 PH, plant height; IL, internode length; SD, stem diameter; FW, fresh weight; LSR, leaf-to-stem ratio; DW, dry weight; LBN, lateral

6 branch number; MBN, main branch number.

**Table 3** (on next page)

Top 10 gene ontology function classification



Table 3 Top 10 gene ontology function classification

Category	Description	GO ID	Count	Percentage(%)
<b>Biological process</b>	translational elongation	GO:0006414	41	4.30
	regulation of protein complex disassembly	GO:0043244	8	0.84
	regulation of translation	GO:0006417	7	0.73
	regulation of translational elongation	GO:0006448	7	0.73
	regulation of translational termination	GO:0006449	7	0.73
	translational frameshifting	GO:0006452	7	0.73
	posttranscriptional regulation of gene expression	GO:0010608	7	0.73
	positive regulation of cellular protein metabolic process	GO:0032270	7	0.73
	regulation of cellular amide metabolic process	GO:0034248	7	0.73
	positive regulation of cellular amide metabolic process	GO:0034250	7	0.73
<b>Cell component</b>	bounding membrane of organelle	GO:0098588	57	5.97
	peptidase complex	GO:1905368	44	4.61
	whole membrane	GO:0098805	49	5.13
	proton-transporting two-sector ATPase complex	GO:0033177	20	2.10
	Golgi apparatus part	GO:0044431	36	3.77
	Golgi apparatus	GO:0005794	36	3.77
	proteasome core complex	GO:0005839	37	3.88
	COPI-coated vesicle membrane	GO:0030126	9	0.94
	COPI-coated vesicle	GO:0030137	9	0.94
COPI vesicle coat	GO:0030126	9	0.94	
<b>Molecular function</b>	translation elongation factor activity	GO:0003746	41	4.30
	translation factor activity, RNA binding	GO:0008135	86	9.01
	acid-amino acid ligase activity	GO:0016881	12	1.26
	UDP-glycosyltransferase activity	GO:0008194	99	1.04
	threonine-type endopeptidase activity	GO:0004298	37	3.88
	threonine-type peptidase activity	GO:0070003	37	3.88
	protein heterodimerization activity	GO:0046982	114	11.95
	ligase activity, forming carbon-nitrogen bonds	GO:0016879	35	3.67
	acetylglucosaminyltransferase activity	GO:0008375	35	3.67
oxidoreductase activity	GO:0016638	12	1.26	

3